Received: 25 April 2019 | Revised: 17 June 2019 | Accepted: 19 June 2019

DOI: 10.1111/cas.14111

ORIGINAL ARTICLE

Cancer Science WILEY

Identification of candidates for driver oncogenes in scirrhous-type gastric cancer cell lines

Eirin Sai[1] | Yoshiyuki Miwa[2] | Reina Takeyama[3,4] | Shinya Kojima[3,4] | Toshihide Ueno[3,4] | Masakazu Yashiro[5] | Yasuyuki Seto[2] | Hiroyuki Mano[3,4]

[1]Department of Medical Genomics, Graduate School of Medicine, The University of Tokyo, Tokyo, Japan

[2]Department of Gastrointestinal Surgery, Graduate School of Medicine, The University of Tokyo, Tokyo, Japan

[3]Department of Cellular Signaling, Graduate School of Medicine, The University of Tokyo, Tokyo, Japan

[4]Division of Cellular Signaling, National Cancer Center Research Institute, Chuo-ku, Tokyo, Japan

[5]Department of Molecular Oncology and Therapeutics, Osaka City University Graduate School of Medicine, Osaka, Japan

Correspondence
Hiroyuki Mano, Division of Cellular Signaling, National Cancer Center Research Institute, 5-1-1 Tsukiji, Chuo-ku, Tokyo 104-0045, Japan.
Email: hmano@ncc.go.jp

Funding information
Japan Agency for Medical Research and Development, Grant/Award Number: JP17am0001001

Abstract

Scirrhous-type gastric cancer (SGC) is one of the most intractable cancer subtypes in humans, and its therapeutic targets have been rarely identified to date. Exploration of somatic mutations in the SGC genome with the next-generation sequencers has been hampered by markedly increased fibrous tissues. Thus, SGC cell lines may be useful resources for searching for novel oncogenes. Here we have conducted whole exome sequencing and RNA sequencing on 2 SGC cell lines, OCUM-8 and OCUM-9. Interestingly, most of the mutations thus identified have not been reported. In OCUM-8 cells, a novel *CD44-IGF1R* fusion gene is discovered, the protein product of which ligates the amino-terminus of CD44 to the transmembrane and tyrosine-kinase domains of IGF1R. Furthermore, both *CD44* and *IGF1R* are markedly amplified in the OCUM-8 genome and abundantly expressed. CD44-IGF1R has a transforming ability, and the suppression of its kinase activity leads to rapid cell death of OCUM-8. To the best of our knowledge, this is the first report describing the transforming activity of IGF1R fusion genes. However, OCUM-9 seems to possess multiple oncogenic events in its genome. In particular, a novel *BORCS5-ETV6* fusion gene is identified in the OCUM-9 genome. *BORCS5-ETV6* possesses oncogenic activity, and suppression of its message partially inhibits cell growth. Prevalence of these novel fusion genes among SGC awaits further investigation, but we validate the significance of cell lines as appropriate reagents for detailed genomic analyses of SGC.

KEYWORDS
BORCS5-ETV6, CD44-IGF1R, fusion kinase, scirrhous-type gastric cancer, tyrosine kinase inhibitor

1 | INTRODUCTION

Despite the advent of screening technologies for the upper digest tract, gastric cancer remains the third leading cause of cancer-related deaths, and almost 1 million people die of this disease worldwide every year.[1,2] In particular, scirrhous-type of gastric cancer (SGC) is one of most intractable cancer subtypes, with a 5-year survival rate of only 11%-16%.[3,4] SGC is characterized by rapid growth and infiltration of poorly differentiated or signet-ring cell-type cancer cells with marked surrounding fibrosis.[5-7] SGC

Sai and Miwa contributed equally to this work.

often lacks apparent mucosal lesions, making it difficult to detect in the early stages.

A wide range of genomic/epigenomic analyses has been conducted to identify therapeutic targets for gastric cancer. By combining whole exome sequencing (WES) and RNA-sequencing (RNA-seq) datasets, for instance, The Cancer Genome Atlas team proposed to divide gastric cancer into 4 subtypes: (i) Epstein-Barr virus-positive type, with a CpG island methylator phenotype and frequent *PIK3CA* nonsynonymous mutations; (ii) microsatellite instability-positive type, with a high mutation burden; (iii) chromosomal instability-positive type with *TP53* alterations and amplification of tyrosine kinase genes; and (iv) genomically stable (GS)-type with frequent mutations within *CDH1*, *RHOA* and *ARID1A*.[8] The GS type is often associated with diffuse-type gastric cancer that significantly overlaps with SGC.

Somatic mutations within *RHOA* were also reported in 14%-25% of diffuse-type gastric cancer.[9,10] Such RHOA mutants are presumed to act in a dominant-negative manner to the wild-type protein, and, thereby, promote cell survival.[11] It is, however, unclear if these *RHOA* mutations are enriched in SGC.

Genome-wide mutation screening with next-generation sequencers (NGS) for SGC is severely hampered by low tumor contents by the markedly increased fibrous tissues in a given specimen. SGC cell lines have been, therefore, useful resources to identify their transforming genes. *FGFR2* gene was, for instance, shown to become amplified and oncogenic in an SGC cell line, KATO-III.[12] *MET* amplification is also reported to be present in some SGC cell lines.[13] To identify potential therapeutic targets in SGC, here we have conducted WES and RNA-seq for 2 SGC cell lines, OCUM-8[14] and OCUM-9. Interestingly, we revealed novel transforming fusion genes, *CD44-IGF1R* from the former cell line and *BORCS5-ETV6* from the latter.

2 | MATERIALS AND METHODS

2.1 | Cell lines

Human embryonic kidney (HEK) 293T cells and mouse 3T3 fibroblasts were obtained from the ATCC (https://www.atcc.org). SGC cell lines, KATO-III and NUGC4, were purchased from Japanese Collection of Research Bioresources (http://cellbank.nibiohn.go.jp/english/). OCUM-1, -2M, -8, -9 and -12 were established by M.Y. All cell lines were maintained in DMEM-F12 medium supplemented with 10% FBS and 2 mmol/L glutamine (all from Invitrogen).

2.2 | Next-generation sequencer analyses

Genomic DNA was isolated from each cell line and subjected to enrichment of exonic fragments with a SureSelect Human All Exon Kit v5 (Agilent) followed by nucleotide sequencing with the HiSeq2500 platform (Illumina) using the paired-end option. Bioinformatics analyses were conducted as reported previously.[15] Nonsynonymous mutations were called only when ≥10% of reads corresponded to the mutations at the positions with a total coverage of ≥20.

Total RNA was isolated from each cell line with the use of an RNeasy Mini Kit (Qiagen) and was subjected to RNA-seq using a NEBNext Ultra Directional RNA Library Prep Kit (New England BioLabs). Relative expression level (fragments per kilobase of exon per million reads mapped, FPKM) of genes were calculated with the Cufflinks pipeline (http://cole-trapnell-lab.github.io/cufflinks/), and fusion genes were searched with deFuse.[16]

2.3 | Cloning of fusion genes

A full-length cDNA of *CD44-IGF1R* was recovered from the RNA of OCUM-8 cells by RT-PCR with the following primers: 5′-TTCGCTCCGGACACCATGGACAAG-3′ and 5′-GATCCAAGGATCAGCAGGTCGAAG-3′. The PCR product was verified with Sanger sequencing. The genomic rearrangement for the *CD44-IGF1R* fusion in OCUM-8 was PCR-amplified from the genomic DNA with the following primers: 5′-TGGACAAGTTTTGGTGGCACGCAG-3′ and 5′-TCACTGGCCCAGGAATGTCATCTG-3′. Genomic PCR or RT-PCR for the *CD44-IGF1R* fusion point was conducted with the genomic primers (5′-ACCCAAGGTCAGGAGTTTGAGACC-3′ and 5′-CACGCTACAATGGACTTCAGTGCC-3′) or the cDNA primers (5′-TTCGCTCCGGACACCATGGACAAG-3′ and 5′-GGCAGAGCGATGATCAGATGGATG-3′), respectively. Similarly, genomic PCR or RT-PCR for *GAPDH* was conducted with the genomic primers (5′-GTCATGGGTGTGAACCATGAGAAG-3′ and 5′-TCTCATACCATGAGTCCTTCCACG-3′) or the cDNA primers (5′-GTCAGTGGTGGACCTGACCT-3′ and 5′-TGAGCTTGACAAAGTGGTCG-3′), respectively. The cDNA of the kinase-dead mutant for CD44-IGF1R was generated with a Site-Directed Mutagenesis Kit (Invitrogen).

Full-length cDNAs of *BORCS5-ETV6* and the wild-type *ETV6* were PCR-amplified using the following primers: 5′-CGTTTCTGTTCCCCAAATAGGGCC-3′ and 5′-GGACTGTTGGTTCCTTCAGCATTC-3′ for the former gene, and 5′-CTCGCTGTGAGACATGTCTGAGAC-3′ and 5′-GGACTGTTGGTTCCTTCAGCATTC-3′ for the latter. The genomic rearrangement for the *BORCS5-ETV6* fusion in OCUM-9 was PCR-amplified with a long-range PCR enzyme (Takara LA Taq, Takara Bio) from the genomic DNA with the following primers: 5′-GACCCAACGATCTGAACTCCTCAG-3′ and 5′-TTTTCAGCCCACTTGAGCCACTGG-3′. Genomic PCR or RT-PCR for the *BORCS5-ETV6* fusion point was conducted with the genomic primers (5′-AAGTCACCATCTGTCCTGGCCTC-3′ and 5′-GAGGGAGCTAAAGCTGGCACAAC-3′) or the cDNA primers (5′-ACGCGTCAGCCCCACACATTAG-3′ and 5′-TTTTCAGCCCACTTGAGCCACTGG-3′), respectively.

2.4 | Functional assay

The cDNA of each gene was ligated into the pMX retroviral vector (Cell Biolabs), and the recombinant vectors were introduced together with an ecotropic packaging plasmid (Takara Bio) into HEK293T cells

to obtain infectious virus particles. For the focus formation assay, 3T3 cells (2×10^6) were infected with ecotropic recombinant retroviruses and cultured for 2 weeks in DMEM-F12 supplemented with 5% calf serum (Invitrogen). For the in vivo tumorigenicity assay, 3T3 cells (5×10^5) expressing each gene were inoculated subcutaneously into nude mice.

To quantitate the copy number of *IGF1R* or *MET*, a part of *IGF1R* or *MET* gene was PCR-amplified with the *IGF1R*-specific primers (5′-GTTCCTGATGAGTGGGAGGT-3′ and 5′-CCCTTGGCAACTCCTTCATA-3′) or the *MET*-specific primers (5′-GCAGAACAAGCTCTCA-3′ and 5′-CCCAGGTGAGTATTTCTC-3′), respectively, by using a droplet digital PCR system (ddPCR; QX200, Bio-rad) with the internal control of *RPP30* gene amplified with the following primers: 5′-GATTTGGACCTGCGAGCG-3′ and 5′-GCGGCTGTCTCCACAAGT-3′.

For immunoblot analyses, cell lysates were obtained from each cell line with the lysis buffer (1% NP-40, 50 mmol/L Tris-HCl, 150 mmol/L NaCl, 1 mmol/L NaF and 1 mmol/L Na_3VO_4). Fifteen micrograms of cell lysates were separated through SDS-PAGE, and probed with antibodies to IGF1R (#9750), phosphorylated IGF1R (#3918), MET (#8198S) or phosphorylated MET (#3077, all from Cell Signaling Technology).

Viable cells were counted with CellTiter-Blue Cell Viability Assay (Promega).

2.5 | Knockdown experiments with shRNA

Nucleotides corresponding to a shRNA against *ETV6* were synthesized based on the shRNA (#sh-9528) from DECIPHER project (http://www.decipherproject.net), and inserted into the pMKO.1-GFP vector, which was a gift from Dr William Hahn (Addgene plasmid #10676; http://n2t.net/addgene:10676; RRID:Addgene_10676). The resultant pMKO.1-sh*ETV6*-GFP allows the simultaneous expression of sh*ETV6* and GFP. The control shRNA sequence is 5′-UGGUUUGCAUGUUGUGUGGCUCGAGUCACA CAACAUGUAAACCA-3′.

The pMKO.1-sh*ETV6*-GFP plasmid together with packaging plasmids (Retrovirus Packaging Kit Ampho, Takara Bio) was transiently transfected into HEK293 cells, and the culture supernatant containing the recombinant retrovirus was used to infect OCUM-9 cells for 2 days. Real-time RT-PCR was conducted with a primer set (5′-TATGAGAAAATGTCCAGAGCCCTG-3′ and 5′-TTCATCCAGCTCCTGGGACTCTAG-3′) for *ETV6*, and with another primer set (5′-GTCAGTGGTGGACCTGACCT-3′ and 5′-TGAGCTTGACAAAGTGGTCG-3′) for *GAPDH*.

2.6 | Accession code

The raw sequencing data have been deposited in the Japanese Genotype-Phenotype Archive (JGA, http://trace.ddbj.nig.ac.jp/jga), which is hosted by DDBJ, under the accession number JGAS00000000179.

3 | RESULTS

3.1 | Genomic analyses of OCUM-8

Whole exome sequencing of the genome of OCUM-8 and -9 was conducted with the mean coverage of 154× and 137×, respectively. More than 96% of exome regions were sequenced at >20× coverage in both cell lines. Messenger RNA was also extensively sequenced with NGS for OCUM-8 and -9, yielding the total nucleotides of 38 and 41 gigabases, respectively.

As shown in Table S1, after excluding nucleotide changes present in our in-house database for normal variations of human genome, we identified a total of 72 nonsynonymous mutations that are present in both exome and RNA-seq datasets of OCUM-8 (with a threshold of total coverage of ≥50× and of the mutation ratio of ≥25% in both datasets). Many of them have not been associated with gastric cancer nor recurrently reported in the COSMIC database version 87 (https://cancer.sanger.ac.uk/cosmic). An exception was the mutation for TP53(E271K) found 37 times in the COSMIC database. The clinical relevance of this mutation is, however, obscure because it is assessed as “Uncertain significance” in the ClinVar database (https://www.ncbi.nlm.nih.gov/clinvar/) as of March 2019.

3.2 | Discovery of a novel fusion gene, *CD44-IGF1R*

Because amplification of *FGFR2* gene and augmentation of tyrosine kinase activity in its protein product plays an essential role in the proliferation of a SGC cell line, KATO-III,[12] we next analyzed chromosome copy number alterations (CNA) in OCUM-8. The high coverage of our WES analysis enabled us to infer detailed CNV, revealing focal amplification of 11p13 and 15q26 loci encompassing *CD44* and *IGF1R* genes, respectively (Figure 1A). We then examined, by quantitative real-time PCR, the copy number of the *IGF1R* gene among control human peripheral blood mononuclear cells and various SGC cell lines, including KATO-III, NUGC4 and OCUM-1, -2M, -8, -9 and -12. As shown in Figure 1B, only OCUM-8 shows a marked amplification of the *IGF1R* gene (copy number = 60) compared to the other samples (mean ± SD = 2.55 ± 0.53). In concordance with this genetic alteration, the expression level of *IGF1R* message is markedly increased in OCUM-8 as well (Figure 1C).

To examine if this genomic alteration produces fusion proteins, we searched for fusion mRNAs among the RNA-seq dataset of OCUM-8. Interestingly, in-frame fusion transcripts were, indeed, found between *CD44* and *IGF1R* and between *IRS2* and *EHF* in OCUM-8 (Table S2). By using RT-PCR, we obtained a full-length *CD44-IGF1R* fusion cDNA from OCUM-8. Nucleotide sequencing of the PCR product revealed that exon 1 of *CD44* becomes fused to exon 12 of *IGF1R* (Figures S1, S2A). Analyses on OCUM-8 genomic DNA further confirmed that chromosome 11 is disrupted at a position 1499 bp-downstream to *CD44* exon 1, and further ligated to a

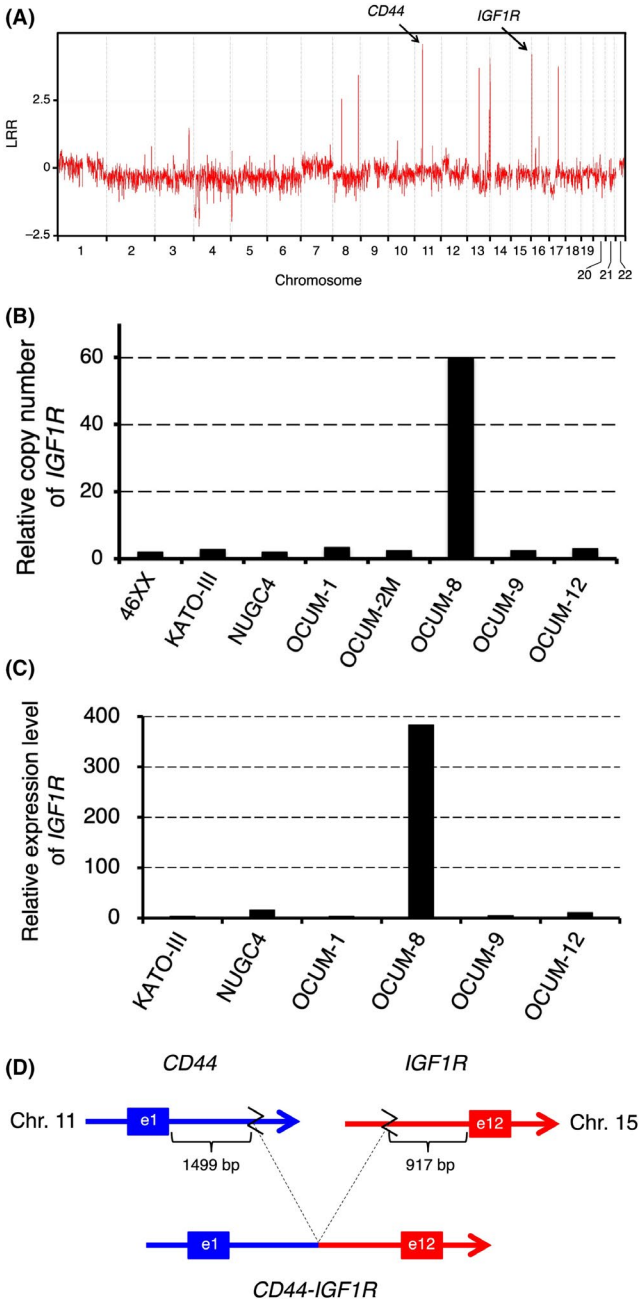

FIGURE 1 Genomic analyses of OCUM-8. A, Chromosome copy number of OCUM-8. From the WES data, the logR ratio (LRR) is calculated and demonstrated. A locus of amplification corresponding to *CD44* or *IGF1R* is indicated. B, The copy number of the *IGF1R* gene compared to that of *RPP30* is examined by using ddPCR among mononuclear cells from peripheral blood of a healthy volunteer (46XX) and scirrhous-type of gastric cancer (SGC) cell lines including KATO-III, NUGC4, OCUM-1, -2M, -8, -9 and -12. The copy number of *IGF1R* in mononuclear cells is set to 2.0. C, Expression level (FPKM) of *IGF1R* is calculated from RNA-seq data of KATO-III, NUGC4, OCUM-1, -8, -9 and -12. D, Genomic PCR with primers placed at exon (e) 1 of *CD44* and at exon 12 of *IGF1R* revealed that *CD44* is disrupted at the position 1499 bp-downstream to exon 1, and ligated to the position 917 bp-upstream to exon 12 of *IGF1R*

nucleotide at 917 bp-upstream to exon 12 of *IGF1R* in chromosome 15 (Figures 1D, S2B, S3). Importantly, the expression of *CD44-IGF1R* gene is driven by the promoter of *CD44* that is known to be abundantly expressed in cancer stem cell fractions.[17]

3.3 | *CD44-IGF1R* is a transforming kinase and therapeutic target in OCUM-8

The *CD44-IGF1R* transcript can encode a chimeric protein of 561 amino acid residues with a predicted molecular weight of 63 386, consisting of the signal peptide of CD44 and the transmembrane and the intracellular domains of IGF1R (Figure 2A). Because fusion proteins of the IGF1R tyrosine kinase domain have rarely been reported, we assessed its transforming activity by using mouse 3T3 fibroblasts.

In the focus formation assay, as demonstrated in Figure 2B, expression of human wild-type CD44 did not induce transformed foci. Forced expression of the wild-type IGF1R induced some phenotypic changes in 3T3 cells but did not yield fully transformed, piled up foci. In contrast, however, induction of CD44-IGF1R resulted in marked transformation in 3T3, as did that of EML4-ALK. In contrast, the kinase-dead mutant of CD44-IGF1R, CD44-IGF1R(KM) in which the lysine residue at amino acid position 227 is replaced with a methionine, failed to produce such transformation, indicating that CD44-IGF1R exerts its oncogenic potential through its elevated tyrosine kinase activity.

The transforming potential of CD44-IGF1R was further confirmed by the nude mouse tumorigenicity assay (Figure 2C). Mouse 3T3 cells expressing each gene were inoculated subcutaneously into nude mice. The cells expressing CD44-IGF1R but not CD44-IGF1R(KM) produced subcutaneous tumors in all injection sites, confirming the oncogenic potential of CD44-IGF1R in vivo.

We further examined if CD44-IGF1R is a therapeutic target for OCUM-8. First, overexpression of the CD44-IGF1R protein in OCUM-8 was confirmed by an immunoblot analysis. Total cell lysates prepared from OCUM-1, KATO-III, OCUM-8 and OCUM-9 were examined with antibodies to the IGF1R protein, revealing that broad bands of 65-90 kDa were detected with the antibody only in OCUM-8 (Figure 2D, left panel). OCUM-8 cells were then incubated with linsitinib, a selective inhibitor against IGF1R tyrosine kinase activity.[18] As shown in the right panel of Figure 2D, immunoblot examination with antibodies to tyrosine-phosphorylated IGF1R revealed that phosphorylation of CD44-IGF1R became decreased with linsitinib in a dose-dependent manner, while the protein amount of CD44-IGF1R was stable with the treatment.

We next investigated whether the enzymatic activity of CD44-IGF1R was essential for the survival of OCUM-8 cells. As demonstrated in Figure 2E, linsitinib strongly and rapidly inhibited the viability of OCUM-8 but did not affect that of CD44-IGF1R-negative OCUM-9 and KATO-III cells.

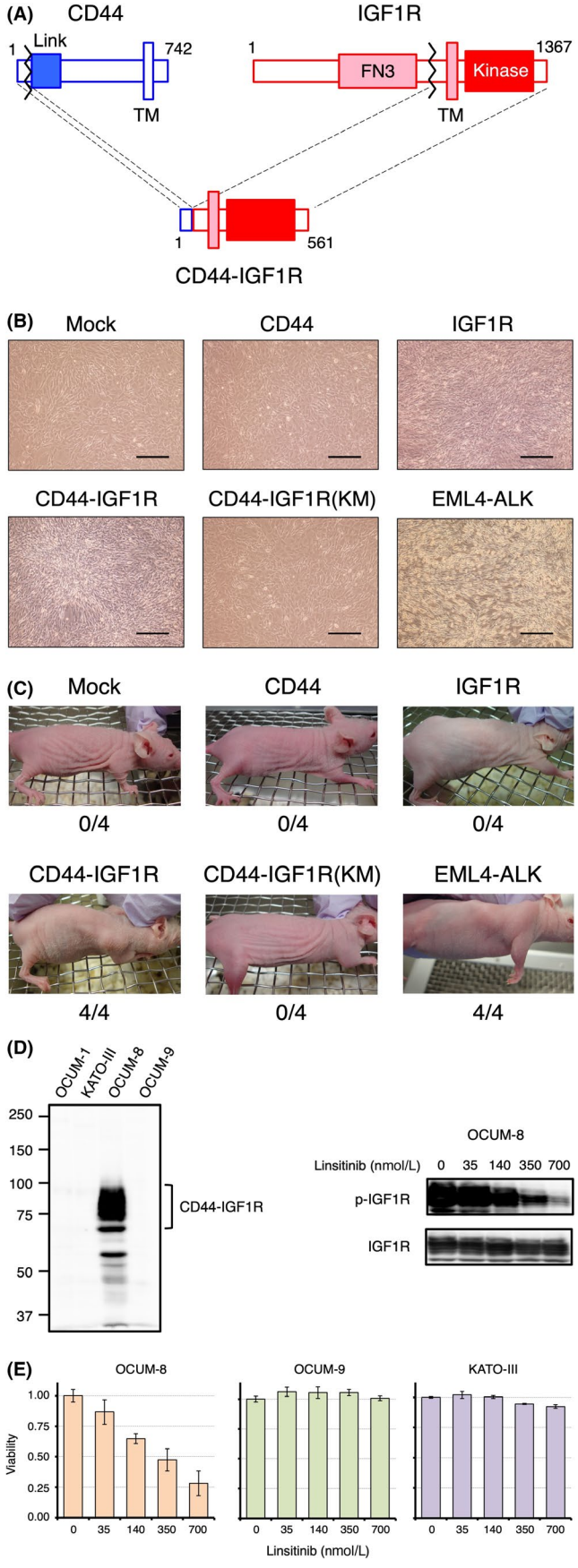

FIGURE 2 Oncogenic activity of CD44-IGF1R fusion kinase. A, The *CD44-IGF1R* cDNA is predicted to encode a protein with the amino-terminal 22 amino acids of CD44 and the carboxyl-terminal 539 amino acids of IGF1R. The LINK, fibronectin type III (FN3) and tyrosine kinase domains are schematically shown. B, Mouse 3T3 fibroblasts were infected with recombinant retrovirus expressing *CD44*, *IGF1R*, *CD44-IGF1R*, *CD44-IGF1R(KM)* or *EML4-ALK*, *or with empty virus (Mock), and cultured for 9 d with 5% calf serum. Scale bar, 100* μm. C, Nude mice were inoculated subcutaneously with the same set of 3T3 cells as in (B), and tumor formation was examined at after 13 d for *EML4-ALK and 16 d for the others. The number of tumors at the injection sites* (*n* = 4) is indicated. D, Total cell lysates (15 μg) were prepared from OCUM-1, KATO-III, OCUM-8 and OCUM-9 cells, separated through SDS-PAGE, and subjected to immunoblot analysis with anti–IGF1R antibodies (left panel). The positions of molecular size standards (in kilodaltons) are indicated at the left of the panel. In the right panel, OCUM-8 cells were treated with different concentrations of linsitinib for 15 min, and their lysates were probed with antibodies to phosphorylated IGF1R (p-IGF1R) or IGF1R. E, OCUM-8, OCUM-9 and KATO-III cells were incubated with different concentrations (shown at the bottom) of linsitinib for 4 h. The elative number of viable cells was calculated with CellTiter-Blue assay, and normalized to that of untreated cells. Data are mean value ± SD of 3 independent experiments

3.4 | *MET* amplification in OCUM-9

Genome profiles of OCUM-9 were also investigated. As depicted in Table S3, a total of 73 nonsynonymous mutations were detected in OCUM-9 with the same threshold from our WES and RNA-seq data. Interestingly, RHOA(L57V) found in OCUM-9 has been already shown to be associated with gastric cancer.[9] While the Leu-to-Val substitution at amino acid position 57 was demonstrated to be loss-of-function, its relevance to gastric cancer remains elusive.

As in the case of OCUM-8, we assessed CNV in the genome of OCUM-9. Focal amplification was detected in chromosomes 2p, 7q and 12p (Figure 3A). Because the 7q locus contains the *MET* gene, we further evaluated the copy number of *MET* with ddPCR among the control cells, KATO-III, NUGC4 and OCUM-1, -2M, -8, -9 and -12 cell lines (Figure 3B). *MET* is highly amplified in OCUM-9 (copy number = 31.4), whereas its amplification (copy number ≥ 4) was not observed in the other samples. The expression level of *MET* was further evaluated by the RNA-seq dataset, revealing its overexpression in OCUM-9 cells (Figure 3C).

Immunoblot analyses with antibodies to MET among OCUM-1, KATO-III, OCUM-8 and OCUM-9 confirmed the overexpression of MET protein (Figure 3D, left panel). In OCUM-9 cells, MET is highly tyrosine-phosphorylated, but such phosphorylation becomes suppressed by the treatment with crizotinib,[19] an inhibitor for MET tyrosine kinase activity (Figure 3D, right panel). Next, OCUM-9 cells were cultured in the presence of crizotinib, showing that crizotinib rapidly inhibited cell viability in a dose-dependent manner (Figure 3E). Crizotinib, in contrast, did not affect that of OCUM-8 and KATO-III. In OCUM-9, MET protein-tyrosine kinase is, thus, a suitable therapeutic target.

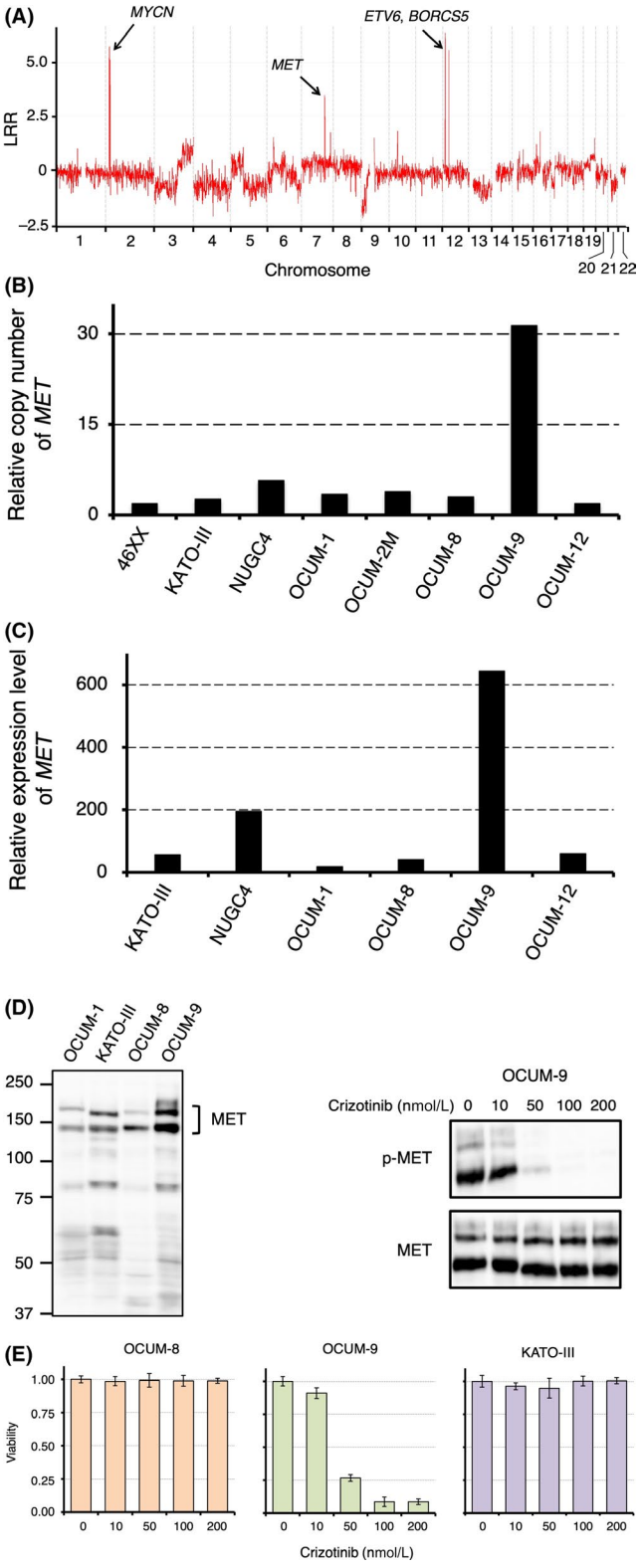

FIGURE 3 Genomic analyses of OCUM-9. A, From the WES data of OCUM-9, the logR ratio (LRR) is calculated as in Figure 1A. An amplification locus corresponding to *MYCN*, *MET or ETV6* plus *BORCS5* is indicated. The copy number (B) and the expression level (C) of *MET* are examined as in Figure 1B,C, respectively. D, Total cell lysates (15 μg) of OCUM-1, KATO-III, OCUM-8 and OCUM-9 were separated through SDS-PAGE, and subjected to immunoblot analysis with anti–MET antibodies (left panel). The positions of molecular size standards (in kilodaltons) are indicated at the left of the panel and that of MET is shown at the right. In the right panel, OCUM-9 cells were treated with different concentrations of crizotinib for 15 min, and their lysates were probed with antibodies to phosphorylated MET (p-MET) or MET. E, OCUM-8, OCUM-9 and KATO-III cells were incubated with different concentrations (shown at the bottom) of crizotinib for 4 h. Relative number of viable cells was calculated with CellTiter-Blue assay, and normalized to that of untreated cells. Data are mean value ± SD of 3 independent experiments

3.5 | Other oncogenic alterations in OCUM-9

As shown in Table S2, OCUM-9 has an in-frame fusion gene between *BORCS5* (also known as *LOH12CR1*) and *ETV6* (Table S2), both of which are localized in the focal amplification locus at chromosome 12p13 (Figure 3A). Based on the estimated copy number gain, this amplicon likely contains *ETV6*, *BCL2L14*, *LRP6*, *MANSC1* and *BORCS5* (Figure 4A). In accordance with the copy number gain, RNA-seq revealed that these genes are abundantly expressed in OCUM-9 cells but not in the other SGC cell lines. It should be noted that genes outside this amplicon are not aberrantly expressed in OCUM-9. Furthermore, the *BORCS5-ETV6* fusion transcript was detected only in OCUM-9 (Figure S4A), and the genomic rearrangement leading to this fusion was further confirmed by genomic analyses (Figure S4B,C).

The predicted *BORCS5-ETV6* message ligates the amino-terminal 20 amino acids of BORCS5 to the majority of ETV6 protein (Figures 4B, S5). To assess the transforming ability of the *BORCS5-ETV6* fusion gene, we conducted the 3T3 focus formation assay. As shown in Figure 4C, both the wild-type ETV6 and BORCS5-ETV6 carry an oncogenic ability when abundantly expressed. Given the high expression of *BORCS5-ETV6* in OCUM-9, this fusion gene likely contributes to OCUM-9 scirrhous cancer development. Indeed, shRNA-mediated knockdown of *ETV6* message partially suppressed the growth of OCUM-9 cells (Figure S6).

Because the focal amplification in chromosome 2p contains the *MYCN* gene, a well-known oncogene, we further examined this amplicon in detail. Copy number estimation reveals that the amplicon contains *NBAS*, *DDX1*, *MYCN* and *MYCNOS* (Figure 4D). Our RNA-seq data, indeed, revealed that these genes are overexpressed only in OCUM-9 cells.

4 | DISCUSSION

Here we have examined oncogenic genomic events in 2 scirrhous-type cancer cell lines, OCUM-8 and OCUM-9, and found *CD44-IGF1R* fusion-type oncogene in the former. *IGF1R* codes for a receptor for type I insulin-like growth factor, which is a transmembrane-type tyrosine kinase. Both IGF1 and IGF2 can bind to and activate the enzymatic potential of IGF1R, and thereby induce a plethora of intracellular signalings. Stimulation of IGF1R can lead to, for instance,

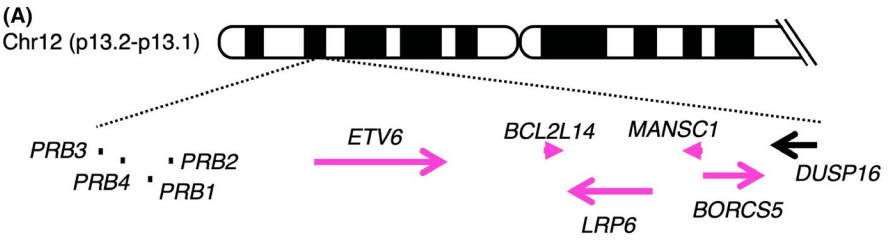

Gene symbol	KATO-III	NUGC4	OCUM-1	OCUM-8	OCUM-9	OCUM-12
PRB1	0.01	0.11	0.03	0.00	0.00	0.00
PRB2	0.00	0.20	0.00	0.00	0.00	0.00
PRB3	0.06	0.01	0.03	0.00	0.00	0.03
PRB4	0.00	0.05	0.00	0.00	0.00	0.00
ETV6	8.71	7.91	7.10	11.41	142.54	9.61
BCL2L14	6.09	3.67	1.38	10.68	3079.76	0.16
LRP6	9.29	10.22	3.38	8.74	1342.80	10.26
MANSC1	40.74	11.82	8.11	27.18	3497.30	15.06
BORCS5	4.96	1.82	2.28	6.34	187.80	4.42
DUSP16	6.56	11.44	3.40	14.91	15.73	25.81

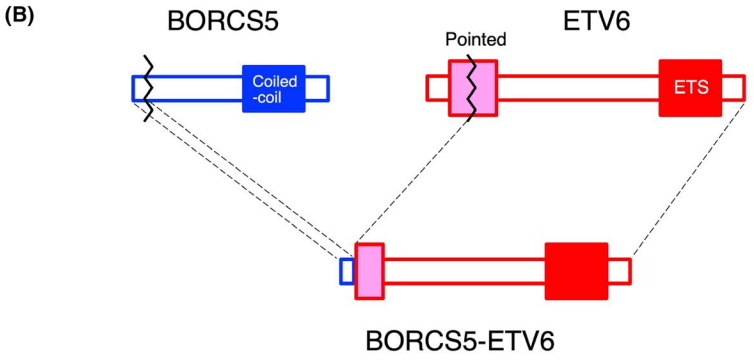

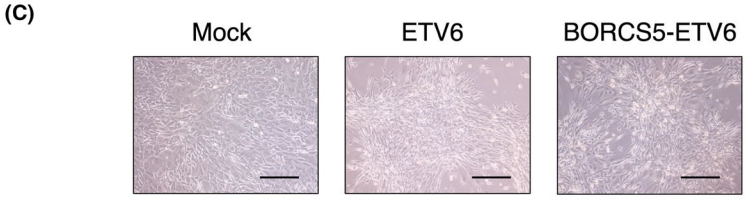

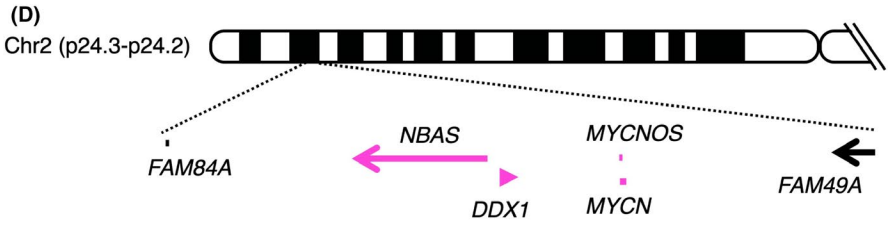

Gene symbol	KATO-III	NUGC4	OCUM-1	OCUM-8	OCUM-9	OCUM-12
FAM84A	3.74	0.63	0.64	0.23	3.11	0.00
NBAS	6.98	4.18	2.84	7.13	144.18	6.17
DDX1	140.20	54.05	38.76	84.47	3005.89	60.95
MYCN	0.47	0.00	0.01	0.05	926.60	0.00
MYCNOS	0.00	0.00	0.00	0.01	120.00	0.00
FAM49A	0.02	0.00	0.01	0.00	0.00	0.01

FIGURE 4 Other oncogenic events of OCUM-9. A, Genes at chromosome 12p13.2 to 12p13.1 are schematically demonstrated, and the genes amplified in OCUM-9 are shown in magenta. The table further demonstrates the expression level (in FPKM) of these genes in KATO-III, NUGC4, OCUM-1, OCUM-8, OCUM-9 and OCUM-12. B, The *BORCS5-ETV6* fusion cDNA can encode a protein with the amino-terminal 20 amino acids of BORCS5 and the carboxyl-terminal 397 amino acids of ETV6. The coiled-coil, Pointed and ETS DNA-binding domains are indicated. C, Mouse 3T3 cells were infected with an empty virus (Mock) or recombinant retrovirus expressing wild-type *ETV6* or *BORCS5-ETV6* fusion gene, and cultured for 7 d. Scale bar, 100 μm. D, Genes at chromosome 2p24.3 to 2p24.2 are schematically shown, and the genes amplified in OCUM-9 are shown in magenta. The expression level of these genes is demonstrated as in (A)

activation of PI3K-AKT-mTOR, RAS-MAPK and IRS2 pathways.[20] IGF1R also has anti–apoptotic ability, and, therefore, is considered to be an appropriate therapeutic target in cancer.[21] Furthermore, IGF1R may play an essential role in acquiring resistance to anti–cancer agents.[22-24]

Although IGF1R overexpression was reported to be a biomarker for drug response or poor outcome, rearrangements of *IGF1R* gene have rarely been reported. Kekeeva et al[25] discovered a fusion transcript of *IGF1R-TTC23* in bladder cancer that encodes the amino-terminal extracellular region of IGF1R fused to TTC23 whose function is yet unknown. Piarulli et al[26] reported on a patient with an ALK-negative inflammatory myofibroblastic tumor carrying *FN1-IGF1R* fusion transcript. Both groups identified *IGF1R* fusion candidates from RNA-seq data but did not confirm the corresponding genomic rearrangements nor examine the transforming ability of the protein products. It should be noted, however, that while the predicted protein product of IGF1R-TTC23 seems not to carry any enzymatic activities, FN1-IGF1R should retain the intracellular tyrosine kinase domain of IGF1R.

In this manuscript, we have validated the genomic rearrangement that fuses the *CD44* and *IGF1R* loci. Because the copy number of both genes are markedly increased (Figure 1A), complex rearrangements involving an amplicon containing *CD44-IGF1R* may take place in the OCUM-8 genome. CD44 is a cell-surface marker for cancer stem cells,[27] and is, indeed, highly expressed in our SGC cell lines (data not shown). In addition, CD44 is involved in the invasion process of SGC cells through the CD44-RAC1 pathway.[28] The promoter of *CD44* should be, therefore, highly active in SGC cells, and may be an ideal partner for *IGF1R* to be in-frame fused. CD44-IGF1R exerts a marked transforming ability in 3T3 cells both in vitro and in vivo, and suppression of its activity in OCUM-8 induces rapid cell death, implying that CD44-IGF1R is an essential growth driver for this cell line. To search for *CD44-IGF1R* in SGC specimens, we further conducted RNA-seq and RT-PCR analyses on formalin-fixed paraffin-embedded tissues from 75 patients with SGC but failed to detect any *IGF1R* fusions among the clinical specimens (data not shown).

In the Tumor Fusion Gene Data Portal (https://tumorfusions.org) where gene fusions can be searched among the data of The Cancer Genome Atlas project, 9 *IGF1R* fusion transcripts are reported as of June 2019 (3 of them are in-frame). Similarly, the cBioPortal database (http://www.cbioportal.org) contains 7 fusion transcripts involving *IGF1R*, and 1 of them is found in stomach adenocarcinoma. Neither database contains the *CD44-IGF1R* fusions. IGF1R may, therefore, directly participate in carcinogenesis at a low frequency.

ETV6 belongs to the ETS family of transcription factors and is known to be fused to potential oncogenes, such as *RUNX1* and *NTRK3*.[29,30] *ETV6* fusion to *BORCS5* has not been reported yet. The focus formation assay revealed that *BORCS5-ETV6* has a transforming ability as the wild-type *ETV6*, although the shape of foci generated by the former seems to be distinct from the latter (Figure 4C). BORCS5 is a component of the BLOC1-related complex, and functions to regulate lysosome localization.[31] Because BORCS5 contains an amino-terminal myristoylation signal,[32] the predicted BORCS5-ETV6 may have an ability to anchor to lipid layer and, thereby, exert oncogenic roles partially different from the wild-type ETV6. The dependency of OCUM9 to *BORCS5-ETV6* for growth further supports the important role of this novel fusion gene in carcinogenesis (Figure S6). Although no fusion transcripts for *BORCS5* are present in the Tumor Fusion Gene Data Portal, 8 *BORCS5* fusions are reported in the cBioPortal (none of them are *BORCS5-ETV6*).

In addition to *BORCS5-ETV6*, however, there are other oncogenic genomic alterations in OCUM-9. The MET tyrosine kinase gene is highly amplified in OCUM-9, and suppression of its enzymatic activity led to rapid cell death (Figure 3A,B, E). Furthermore, *MYCN* is markedly amplified and expressed in the same cell line (Figures 3A and 4D). Importantly, amplification of *MYCN* is frequently found in neuroblastoma,[33] and the forced expression of *MYCN* in dopamine β-hydroxylase-expressing cells in mice is sufficient to induce tumors resembling human neuroblastoma.[34] It is, therefore, likely that multiple oncogenic events contribute to the generation of OCUM-9.

We here reported novel oncogenic alterations in gastric cancer, *IGF1R*-fusion and *ETV6*-fusion genes, prevalence of which awaits further investigation. Detailed examination of other SGC cell lines may further decipher the molecular mechanisms underlying SGC and provide us therapeutic targets in this highly intractable malignancy.

CONFLICTS OF INTEREST

The authors declare no conflicts of interest for this article.

ORCID

Masakazu Yashiro https://orcid.org/0000-0001-5743-7228
Hiroyuki Mano https://orcid.org/0000-0003-4645-0181

REFERENCES

1. Wadhwa R, Song S, Lee JS, Yao Y, Wei Q, Ajani JA. Gastric cancer-molecular and clinical dimensions. *Nat Rev Clin Oncol*. 2013;10:643-655.
2. Bray F, Ferlay J, Soerjomataram I, Siegel RL, Torre LA, Jemal A. Global cancer statistics 2018: GLOBOCAN estimates of incidence and mortality worldwide for 36 cancers in 185 countries. *CA Cancer J Clin*. 2018;68:394-424.
3. Chen CY, Wu CW, Lo SS, Hsieh MC, Lui WY, Shen KH. Peritoneal carcinomatosis and lymph node metastasis are prognostic indicators in patients with Borrmann type IV gastric carcinoma. *Hepatogastroenterology*. 2002;49:874-877.
4. Japanese Gastric Cancer Association Registration C, Maruyama K, Kaminishi M, et al. Gastric cancer treated in 1991 in Japan: data analysis of nationwide registry. *Gastric Cancer*. 2006;9:51-66.
5. Ikeguchi M, Miyake T, Matsunaga T, et al. Recent results of therapy for scirrhous gastric cancer. *Surg Today*. 2009;39:290-294.

6. Yashiro M, Hirakawa K. Cancer-stromal interactions in scirrhous gastric carcinoma. *Cancer Microenviron*. 2010;3:127-135.
7. Yashiro M, Matsuoka T, Ohira M. The significance of scirrhous gastric cancer cell lines: the molecular characterization using cell lines and mouse models. *Hum Cell*. 2018;31:271-281.
8. Cancer Genome Atlas Research N. Comprehensive molecular characterization of gastric adenocarcinoma. *Nature*. 2014;513:202-209.
9. Wang K, Yuen ST, Xu J, et al. Whole-genome sequencing and comprehensive molecular profiling identify new driver mutations in gastric cancer. *Nat Genet*. 2014;46:573-582.
10. Kakiuchi M, Nishizawa T, Ueda H, et al. Recurrent gain-of-function mutations of RHOA in diffuse-type gastric carcinoma. *Nat Genet*. 2014;46:583-587.
11. Nishizawa T, Nakano K, Harada A, et al. DGC-specific RHOA mutations maintained cancer cell survival and promoted cell migration via ROCK inactivation. *Oncotarget*. 2018;9:23198-23207.
12. Ueda T, Sasaki H, Kuwahara Y, et al. Deletion of the carboxyl-terminal exons of K-sam/FGFR2 by short homology-mediated recombination, generating preferential expression of specific messenger RNAs. *Cancer Res*. 1999;59:6080-6086.
13. Kuniyasu H, Yasui W, Kitadai Y, Yokozaki H, Ito H, Tahara E. Frequent amplification of the c-met gene in scirrhous type stomach cancer. *Biochem Biophys Res Commun*. 1992;189:227-232.
14. Takemura S, Yashiro M, Sunami T, Tendo M, Hirakawa K. Novel models for human scirrhous gastric carcinoma in vivo. *Cancer Sci*. 2004;95:893-900.
15. Sato K, Kawazu M, Yamamoto Y, et al. Fusion kinases identified by genomic analyses of sporadic microsatellite instability-high colorectal cancers. *Clin Cancer Res*. 2019;25:378-389.
16. McPherson A, Hormozdiari F, Zayed A, et al. deFuse: an algorithm for gene fusion discovery in tumor RNA-Seq data. *PLoS Comput Biol*. 2011;7:e1001138.
17. Ishimoto T, Nagano O, Yae T, et al. CD44 variant regulates redox status in cancer cells by stabilizing the xCT subunit of system xc(-) and thereby promotes tumor growth. *Cancer Cell*. 2011;19:387-400.
18. Fassnacht M, Berruti A, Baudin E, et al. Linsitinib (OSI-906) versus placebo for patients with locally advanced or metastatic adrenocortical carcinoma: a double-blind, randomised, phase 3 study. *Lancet Oncol*. 2015;16:426-435.
19. Zou HY, Li Q, Lee JH, et al. An orally available small-molecule inhibitor of c-Met, PF-2341066, exhibits cytoreductive antitumor efficacy through antiproliferative and antiangiogenic mechanisms. *Cancer Res*. 2007;67:4408-4417.
20. Iams WT, Lovly CM. Molecular pathways: clinical applications and future direction of insulin-like growth factor-1 receptor pathway blockade. *Clin Cancer Res*. 2015;21:4270-4277.
21. LeRoith D, Helman L. The new kid on the block(ade) of the IGF-1 receptor. *Cancer Cell*. 2004;5:201-202.
22. Lovly CM, McDonald NT, Chen H, et al. Rationale for co-targeting IGF-1R and ALK in ALK fusion-positive lung cancer. *Nat Med*. 2014;20:1027-1034.
23. Zorea J, Prasad M, Cohen L, et al. IGF1R upregulation confers resistance to isoform-specific inhibitors of PI3K in PIK3CA-driven ovarian cancer. *Cell Death Dis*. 2018;9:944.
24. Loganathan SN, Tang N, Holler AE, Wang N, Wang J. Targeting the IGF1R/PI3K/AKT pathway sensitizes Ewing sarcoma to BET bromodomain inhibitors. *Mol Cancer Ther*. 2019;18:929-936.
25. Kekeeva T, Tanas A, Kanygina A, et al. Novel fusion transcripts in bladder cancer identified by RNA-seq. *Cancer Lett*. 2016;374:224-228.
26. Piarulli G, Puls F, Wangberg B, et al. Gene fusion involving the insulin-like growth factor 1 receptor in an ALK-negative inflammatory myofibroblastic tumour. *Histopathology*. 2019;74:1098–1102.
27. Prince ME, Sivanandan R, Kaczorowski A, et al. Identification of a subpopulation of cells with cancer stem cell properties in head and neck squamous cell carcinoma. *Proc Natl Acad Sci USA*. 2007;104:973-978.
28. Satoyoshi R, Kuriyama S, Aiba N, Yashiro M, Tanaka M. Asporin activates coordinated invasion of scirrhous gastric cancer and cancer-associated fibroblasts. *Oncogene*. 2015;34:650-660.
29. Wlodarska I, Mecucci C, Baens M, Marynen P, van den Berghe H. ETV6 gene rearrangements in hematopoietic malignant disorders. *Leuk Lymphoma*. 1996;23:287-295.
30. Lannon CL, Sorensen PH. ETV6-NTRK3: a chimeric protein tyrosine kinase with transformation activity in multiple cell lineages. *Semin Cancer Biol*. 2005;15:215-223.
31. Pu J, Schindler C, Jia R, Jarnik M, Backlund P, Bonifacino JS. BORC, a multisubunit complex that regulates lysosome positioning. *Dev Cell*. 2015;33:176-188.
32. Utsumi T, Sato M, Nakano K, Takemura D, Iwata H, Ishisaka R. Amino acid residue penultimate to the amino-terminal gly residue strongly affects two cotranslational protein modifications, N-myristoylation and N-acetylation. *J Biol Chem*. 2001;276:10505-10513.
33. Schwab M, Varmus HE, Bishop JM, et al. Chromosome localization in normal human cells and neuroblastomas of a gene related to c-myc. *Nature*. 1984;308:288-291.
34. Althoff K, Beckers A, Bell E, et al. A Cre-conditional MYCN-driven neuroblastoma mouse model as an improved tool for preclinical studies. *Oncogene*. 2015;34:3357-3368.

SUPPORTING INFORMATION

Additional supporting information may be found online in the Supporting Information section at the end of the article.

How to cite this article: Sai E, Miwa Y, Takeyama R, et al. Identification of candidates for driver oncogenes in scirrhous-type gastric cancer cell lines. *Cancer Sci*. 2019;110:2643-2651. https://doi.org/10.1111/cas.14111